JOURNAL OF MATERIALS SCIENCE 23 (1988) 281–287

Notched bend tests on WC–Co hardmetals

B. ROEBUCK
National Physical Laboratory, Teddington, Middlesex TW11 0LW, UK

Notched bend tests have been performed on a range of WC–Co hardmetals. The notch stress concentration factors were derived from conventional notch stress analysis and by a finite-element method. The introduction of the notch suppressed the initiation of failures from macroscopic defects such as pores and inclusions. The strength values obtained were thus representative of the underlying hardmetal microstructure.

1. Introduction

Previous work [1] has shown that bend tests on hardmetals can be analysed to provide information, both on strength values when failures are initiated from macroscopic defects and, in the absence of such defects, a limiting strength. The latter property can be measured in tests in which the most highly-stressed volume is small, thus reducing the likelihood of encountering large defects. A chamfered bend test specimen was developed [2] to obtain limiting strength values from a small number of specimens. A theoretical analysis [3] of the chamfered bend test specimens and other geometries showed that a triangular-shaped test piece was probably the most efficient for localizing the stress. However, there are practical limitations in preparing either chamfered or triangular test-pieces. In the present work the effect of notching bent-test specimens has been examined to see if the same principle of minimizing the most highly-stressed volume could be achieved in a test-piece geometry which was simpler to prepare. The introduction of a notch has an additional benefit in that its presence results in lower nominal applied breaking loads. Thus high-load-capacity machines are not required and the damage to bending rigs as a result of test-piece fragmentation during specimen failure is minimized.

Notches of different depths were produced with a profiled diamond grinding wheel to ensure a constant notch radius. The stress concentration factor for each notch was estimated by conventional notch stress analysis and also by using finite-element analysis. The stress concentration factors obtained by each of these methods were in reasonably close agreement.

The strength values obtained from the notched specimens were compared with the results of previous tests [1] on chamfered specimens. Also, since the grinding process had been shown [2] to introduce residual stresses [1] which affected the nominal values of limiting strength, the effects of grinding were examined by testing specimens in the as-ground and ground and annealed conditions.

In analysing the results a proportion of the broken test-pieces were examined by scanning electron fractography to ascertain the nature of the failure initiation site. The purpose of the examination was to see if the failure site corresponded to a limiting strength value.

2. Materials and testing details

Tests were performed on six WC–Co hardmetals. Details of their properties are given in Table I, where the hardmetals are referred to as 6VF, 6F, 6C, 10VF, 11F and 11C according to their cobalt content in wt % and WC grain-size: very fine (VF), fine (F) and coarse (C). All the samples were free from eta-phase or graphite. Samples 6VF and 10VF contained 1.5 and 2 wt % (Ta, Nb)C, respectively, as a grain-size inhibitor.

The bend tests were performed in a three-point bend rig which conformed with the current standard [4] for transverse rupture testing of hardmetals. The span of the rig was 14 mm. The dimensions of the test-pieces are given in Table II. The specimens were ground parallel to the length direction with a well-lubricated diamond resin-bonded wheel. No pass exceeded 0.01 mm. The deviation from parallelism was less than 0.01 mm on opposite faces. The dimensions of each specimen were measured to an accuracy of ± 0.01 mm.

The notch depths were of three sizes: 2, 1 and 0.5 mm. A profiled V-notch diamond resin-bonded wheel was used to grind the notches, removing about 0.002 mm per pass. The radius of the root of the finished notch was 0.5 mm and the included angle between the faces of the notch was 90°.

A proportion of the notched specimens were annealed, prior to testing, for 1 h at 800° C in a vacuum. The bend tests were all performed at room temperature, approximately 20° C, and the load was applied at a rate of about 50 N sec^{-1}.

3. Results

3.1. Notch stress analysis

A schematic diagram of the notched bend specimens is shown in Fig. 1. M is the bending moment. The nominal stress at Point A in an unnotched specimen, σ_A, is given by

$$\sigma_A = \frac{6M}{bh^2} \quad (1)$$

where M is the bending moment. The stress at Point B, σ_B, is given by

$$\sigma_B = K\frac{6M}{by^2} \quad (2)$$

0022–2461/88 $03.00 + .12

TABLE I Physical properties of hardmetals

Sample	Co (wt %)	Carbide grain size* (μm)	Hardness, HV30	Magnetic moment ($\mu T m^3 kg^{-1}$)	Coercivity ($kA m^{-1}$)
6VF	6	0.57	1765	0.70	25.0
6F	6	1.44	1540	0.87	14.5
6C	6	4.81	1235	0.87	6.0
10VF	10	0.57	1565	1.37	20.0
11F	11	1.41	1330	1.58	10.5
11C	11	5.12	1100	1.58	4.5

*1.5 × mean linear intercept.

where K is a geometrical factor. Thus

$$\sigma_B = K\frac{h^2}{y^2}\sigma_A \quad (3)$$

Values for the factor K were obtained from Engineering Sciences Data Unit sheets (ESDU 69020) and are given in Table III. It was assumed that the magnitude of the stress concentration factors associated with the V-notch were similar to those of the U-notches in the Data Unit sheets.

3.2. Finite-element analysis

In three-point bend tests on specimens with a short span to height ratio a wedging action results in a maximum nominal stress which is greater than the true stress by an amount which depends on the height to span ratio, h/s. The maximum stress corrected for wedging, σ_w, in unnotched specimens is given [5] by

$$\sigma_w = \frac{3Ps}{2bh^2}\left(1 - \frac{4h}{3\pi s}\right) \quad (4)$$

where P is the applied load and s is the span of the three-point bend rig. Because of this effect, which is about 10 to 15% for the dimensions of hardmetal standard transverse rupture-test specimens, a finite-element analysis was performed as an additional check on the conventional notch stress analysis.

The finite-element analysis was performed with a commercially available program (PAFEC 75) on a mainframe ICL 2972 computer. The analysis was performed on the full beams of unit width for unnotched and notched specimens (1 mm and 2 mm deep) with s and h set at 14 and 4.4 mm, respectively. The meshes and exaggerated displacements under unit applied loads are shown in Fig. 2 for each of these three specimens. The analysis was performed by fixing the position of the central loading point in space and constraining the plane through this point to remain in the same plane. Equal loads were applied at two equidistant positions 7 mm from the centre on the lower edge.

Maximum principal stress contours for each of the loaded specimens are shown in Fig. 3 and the values obtained for the principal stresses are given in Table IV.

The values shown in Table IV indicate that the stress concentration factors obtained by the stress analysis and the finite-element method were in reasonably good agreement. The directions of the maximum principal stresses given in Table IV were within 1 to 2° of the longitudinal direction in the beam.

A plot of maximum principal stress against position along the tensile surface of the unnotched beam obtained by finite-element analysis is shown in Fig. 4. The plot shows very clearly the effect of the wedging action, due to the short span to height ratio, in reducing the magnitude of the stress compared to the value calculated from the nominal stress formula.

The choice of mesh geometry and size is an important consideration to be taken into account in performing the finite-element analysis. The meshes shown in Fig. 2 were chosen as the most convenient from those available. However, an additional calculation was performed on the sample geometry with a 2 mm deep notch in which the mesh size in the vicinity of the notch was reduced by a factor of about 2. The maximum principal stress was calculated to be about 12.5 $kN mm^{-2}$ compared with a value of 11.5 $kN mm^{-2}$ obtained with a less-refined mesh size. The stress concentration factor was thus 12.5/2.07 = 6.05 which was in very good agreement with the value of 6.2 obtained for the stress concentration factor from the conventional notch stress analysis.

3.3. Notched bend tests

The results of the notched bend tests are summarized in Table V and shown in Figs 5 and 6.

Fig. 5 shows that the failure loads increase with decreasing notch depth, reflecting the diminishing value of stress concentration factor with the latter. It

TABLE II Notched bend test-piece dimensions

Sample	Specimen height, h (mm)	Specimen width, b (mm)	Notch depth, d (mm)
6VF	6.3 to 6.5	2	2
6VF	4.5	2	0.5
6F	4.5	2.5	2, 1 and 0.5
6C	4.5	2.5	2, 1 and 0.5
10VF	6.3 to 6.5	2	2
10VF	4.5	2	0.5
11F	4.5	2.5	2, 1 and 0.5
11C	4.5	2.5	2, 1 and 0.5

TABLE III Notch stress analysis

Sample dimensions (mm)			K*	$\sigma_B/\sigma_A^\dagger$
h	y	d		
4.5	4	0.5	2.1	2.7
4.5	3.5	1.0	2.2	3.6
4.5	2.5	2.0	1.9	6.2
6.25	4.25	2.0	2.35	5.1
6.5	4.5	2.0	2.45	5.1

*The uncertainty in K is about ±0.05.
†Rounded to nearest 0.1.

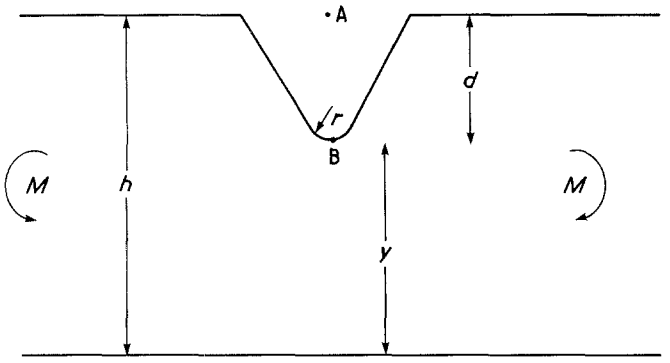

Figure 1 Schematic diagram of notch.

is also clear that the nominal failure load for all the specimens is largest in the as-ground specimens. Previous work [2] has shown that this can be accounted for by the presence of residual compressive stresses present as a result of the grinding process. There was more scatter in properties for the shallowest of the notch depths, 0.5 mm. This scatter might have been caused by the uncertainty in notch depth which, as a percentage value, was greatest for the shallowest notch.

The stress concentration factors obtained from the conventional notch analysis were used to convert the nominal failure loads to failure stresses. The results are plotted in Fig. 6 as average values and several observations can be made.

(a) The failure stress was essentially independent of notch depth, and all the specimens showed reasonably consistent strength values, particularly the coarse-grained specimens.

(b) The effects of grinding can be seen to increase the value of nominal failure stress. The apparent increase in failure stress was slightly smaller for the coarser-grained samples.

(c) The failure stress of the annealed specimens was almost independent of composition. Previous work [3] on chamfered specimens had reached the same conclusion.

(d) Also shown in Fig. 6 for comparison are the results obtained in earlier work [2] on chamfered specimens. There was very good agreement between the failure stresses obtained in both the as-ground and as-ground and annealed notched bend specimens and the chamfered specimens. The good agreement supports the values used for the stress consentration factors.

(e) The results obtained on the very-fine-grained hardmetals appeared to fall into two groups dependent on the specimen height, h. The strength values obtained on samples with specimen height, h, of equal value, 4.5 mm, to the other specimens were about 2.4 to 2.5 $kN\,mm^{-2}$ and similar to those of the latter. However, the other samples of 6VF and 10VF with specimen heights, h, equal to either 6.3 or 6.5 mm had slightly higher strength values. A possible reason for the difference might be that the results shown in Fig. 6 do not allow for the wedging effect (Equation 4). This effect results in the true stress value being overestimated as shown in Fig. 4. The effect increases with specimen height. The correction factor for 4.5 mm deep specimens is about 14% compared with 20% for 6.5 mm deep specimens (Equation 4). Consequently, making allowance for the effect would result in closer agreement between the calculated failure stress values for the 6.3 to 6.5 and 4.5 mm high specimens. A

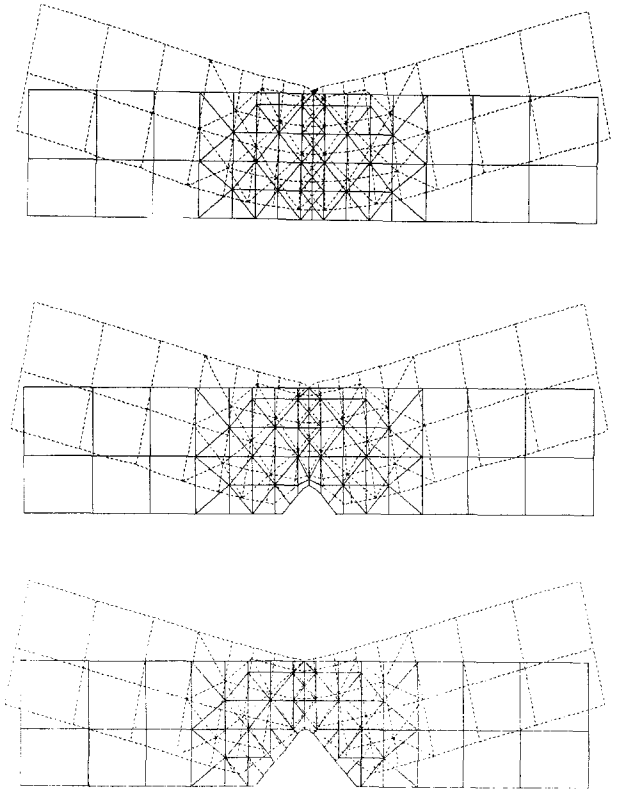

Figure 2 Finite element meshes.

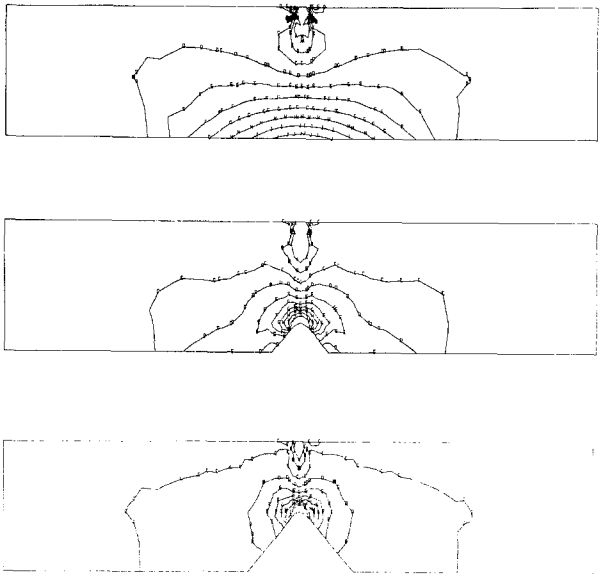

Figure 3 Maximum principal stress contours.

TABLE IV Finite-element analysis

Specimen dimensions (mm)			Principal stresses* ($kN\,mm^{-2}$)		Stress concentration factor	
h	y	d	Maximum	Minimum	Finite-element analysis	Conventional notch analysis
4.4	0	0	+2.07	-0.2×10^{-4}	–	–
4.4	3.4	1.0	+7.05	−0.1	3.4	–
4.5	3.5	1.0	–	–	–	3.6
4.4	2.4	2.0	+11.5	+0.84	5.6	–
4.5	2.5	2.0	–	–	–	6.2

*Positive stresses are tensile, negative stresses are compressive. The values for the unnotched specimen are at the beam centre beneath the loading point and for the notched specimens at the notch root.

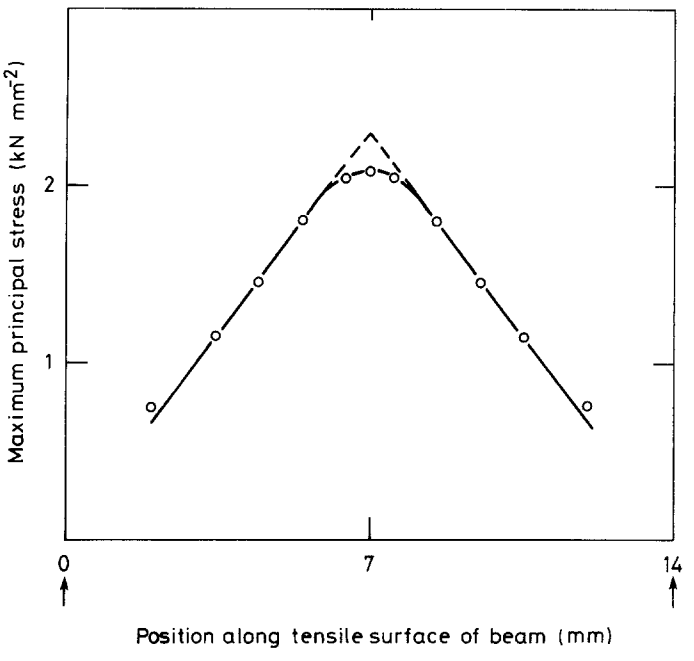

Figure 4 Maximum principal stress against position (unnotched beam): (○) finite-element analysis, (– – –) nominal stress.

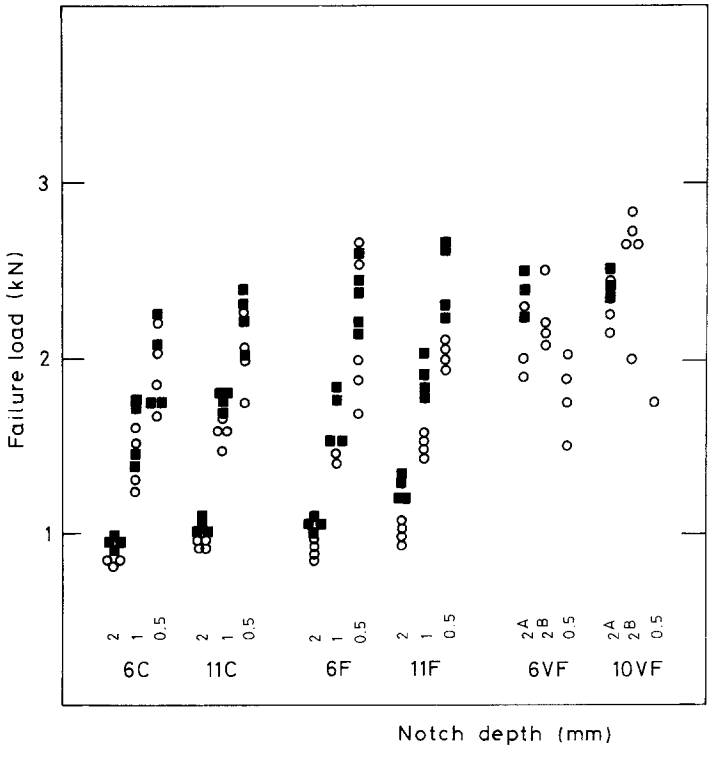

Figure 5 Failure load against notch depth: (■) as-ground, (○) annealed. W = 6.3 mm at A, 6.5 mm at B.

TABLE V Notched bend tests

Sample	Sample* preparation	Notch depth (mm)	Specimen height, h (mm)	Average failure load (N)	Average failure stress† ($N mm^{-2}$)	Number
6F	G	2	4.5	1055	2715	4
6F	A	2	4.5	912	2345	4
6F	G	1	4.5	1678	2505	4
6F	A	1	4.5	1480	2210	2
6F	G	0.5	4.5	2364	2645	5
6F	A	0.5	4.5	2178	2440	5
11F	G	2	4.5	1265	3250	4
11F	A	2	4.5	1009	2595	4
11F	G	1	4.5	1910	2850	4
11F	A	1	4.5	1510	2255	4
11F	G	0.5	4.5	2475	2770	4
11F	A	0.5	4.5	2033	2275	4
6C	G	2	4.5	961	2470	4
6C	A	2	4.5	827	2130	4
6C	G	1	4.5	1585	2365	4
6C	A	1	4.5	1425	2130	4
6C	G	0.5	4.5	1965	2200	4
6C	A	0.5	4.5	1963	2195	4
11C	G	2	4.5	1009	2595	4
11C	A	2	4.5	912	2345	4
11C	G	1	4.5	1759	2625	4
11C	A	1	4.5	1580	2360	4
11C	G	0.5	4.5	2278	2550	4
11C	A	0.5	4.5	2053	2300	4
6VF	G	2	6.3	2380	3210	3
6VF	A	2	6.3	2070	2790	3
6VF	A	2	6.5	2240	2835	4
6VF	A	0.5	4.5	1790	2505	4
10VF	G	2	6.3	2460	3320	3
10VF	A	2	6.3	2310	3115	3
10VF	A	2	6.5	2590	3280	5
10VF	A	0.5	4.5	1750	2450	1

*G: as-ground, A: annealed.
†Calculated using stress concentration factors from Table III for notch analysis. Rounded to nearest $5 N mm^{-2}$.

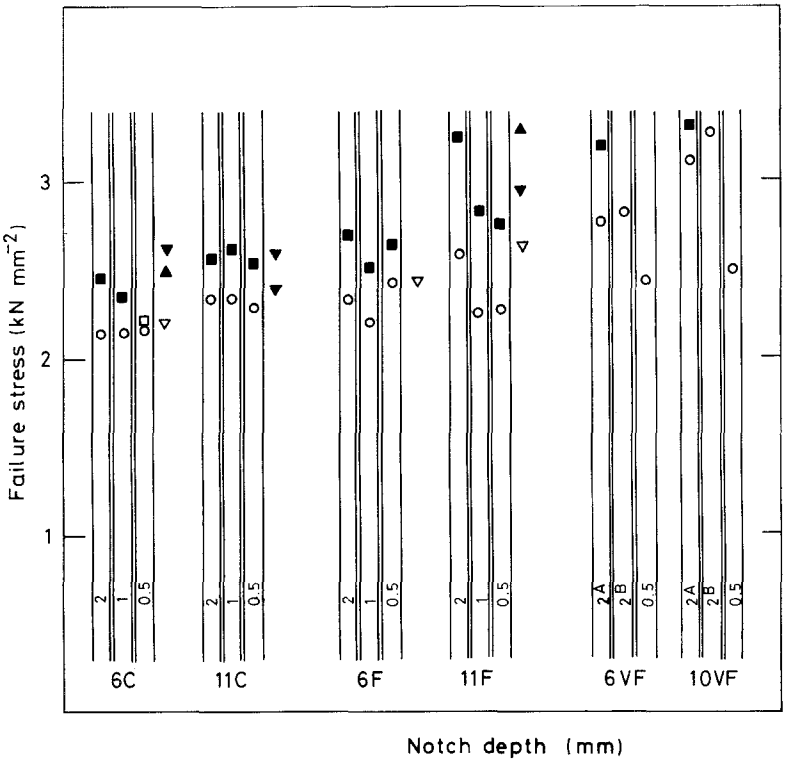

Figure 6 Failure stress against notch depth: (■, ▲) ground transverse; (▼) ground longitudinally; (○, ▽) annealed; (▽, ▼, ▲) chamfered; (○, ■) notched. W = 6.3 mm at A, 6.5 mm at B.

correction factor could be provided by the finite-element method. However the latter was only performed for 2 mm deep notches in the 4.5 mm height specimens and so would need, in addition, to be repeated on the 6.3 to 6.5 mm height samples with a 2 mm deep notch for quantitative confirmation of this explanation.

3.4. Fractography

123 notched bend specimens were tested and about 70% were examined by scanning electron fractography to identify the fracture origin. Four of the examined samples failed from pores (Fig. 7a) and three from clusters of WC grains (Fig. 7b). One of the 10VF samples failed from a very large pore with a breaking load of 1350 N. This load was considerably smaller than the breaking load of the other 10VF sample (1750 N) which had no obvious fracture origin. The result from the sample of 10VF with the breaking load of 1350 N was excluded from the Table V and Fig. 5. The results from the other six samples with obvious failure origins were included in Fig. 5 and Table V since the breaking loads did not appear to be significantly different from those of the other samples with comparable notch geometrics. Previous work [2] had shown that for small defects the effective limiting stress was defect-size-independent. It is thus likely that the defects in these six samples were at, or close to, this limit. More samples would need to be tested to examine the statistical significance of defect-initiated failures from a larger number of specimens. However, since the notch geometry minimizes the chance of failure arising from gross defects it is likely that a very large number, possibly as many as 1000, of specimens would need to be tested. A proportion of the samples also failed from the corner between the edge of the specimen and the notch root. However, a large majority (about 75%) of the examined specimens failed from regions in which no obvious defect could be seen (Figs 8a and b) and were classed as microstructurally-initiated.

4. Conclusions

Limiting strength values for hardmetals can be obtained from notched bend test samples.

The stress concentration factor for a variety of notch depths was obtained by a conventional notch stress analysis. A finite-element analysis confirmed that the values of stress concentration factor obtained by the conventional stress analysis were reasonably accurate.

The limiting strength values obtained from the

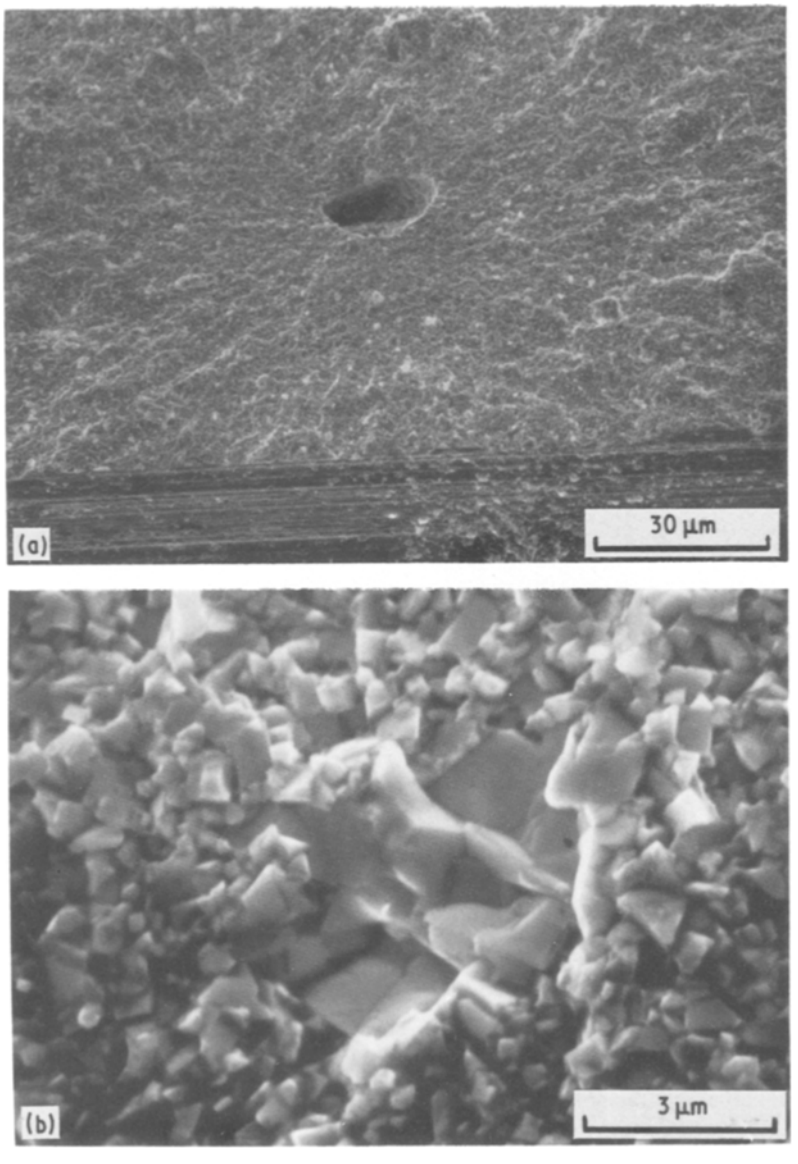

Figure 7 (a) Pore, (b) WC cluster.

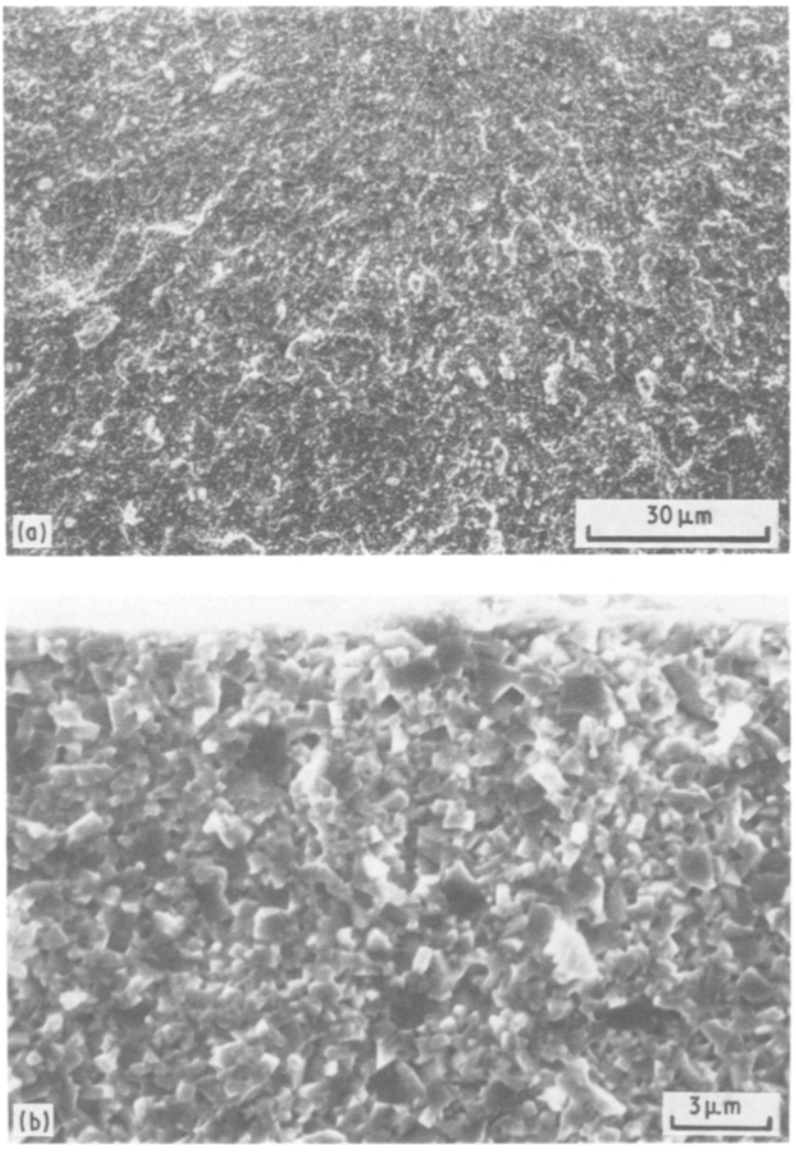

Figure 8 (a, b) Microstructurally initiated, no obvious flaw or defect.

notched samples were similar to results obtained in previous tests on chamfered specimens. The tests confirmed that for a wide range of hardmetals the tensile or limiting strength of microstructurally-initiated broken bend specimens did not vary to a large degree as the WC grain size or cobalt volume fraction were altered. Also, strength was significantly increased by the presence of grinding stresses.

Acknowledgements

Part financial support was provided by a European Community R and D programme in the Raw Materials Sector: Substitution and Ceramics. Samples were provided by Wimet Ltd and Ledermann Gmbh.

References

1. E. A. ALMOND and B. ROEBUCK, *Met. Sci.* **11** (1977) 458.
2. B. ROEBUCK, *J. Mater. Sci.* **14** (1979) 2837.
3. M. G. GEE, *Res Mechanica* **4** (1982) 295.
4. "Hardmetals – Determination of Transverse Rupture Strength", ISO 3327, 2nd Edn (1982).
5. S. TIMOSHENKO, in "Strength of Materials", 3rd Edn edited by R. F. Kreiger (New York, 1976) pp. 57–59.

Received 19 March
and accepted 15 May 1987